Role of bianisotropy in negative permeability and left-handed metamaterials

Ricardo Marqués,* Francisco Medina,† and Rachid Rafii-El-Idrissi

Dpto. Electrónica y Electromagnetismo, Facultad de Física, Univ. de Sevilla, Avda. Reina Mercedes s/n, 41012-Sevilla, Spain
(Received 9 November 2001; published 4 April 2002)

The recently proposed artificial media with negative magnetic permeability and left-handed metamaterials are revisited at the light of the theory of artificial bi(iso/aniso)tropic media. In particular, the existence of bianisotropic effects in those materials is investigated, making use of an approximate model. Some unexplained properties of the electromagnetic-wave propagation through these media, revealed by closer inspection of previous numerical simulations and experimental work, are highlighted. It is shown that these peculiarities are properly explained if the bianisotropy is explicitly accounted for. The bianisotropy is related to the existence of magnetoelectric coupling in the artificial constituents (artificial atoms) of the medium. A simple modification of the artificial atom that precludes the bianisotropy is also proposed.

I. INTRODUCTION

A material medium consisting of metallic inclusions randomly or periodically distributed inside a host dielectric behaves, at least within a certain range of frequencies (typically in the microwave region), as an effective continuous medium whose electromagnetic constitutive parameters may have values well outside of the range covered by ordinary materials. Thus, for instance, an artificial negative electric permittivity medium (NEPM) can be obtained by using long metallic wires as inclusions,[1,2] which simulate the plasma behavior at microwave frequencies. Since free magnetic charges are not present in nature, this method cannot be used for manufacturing negative magnetic permeability media (NMPM). Such media, however, can be built up by using small resonant metallic *particles* with very high magnetic polarizability. Recently, a particle having this property, the so-called *split ring resonator* (SRR), has been proposed for this purpose.[3] An artificial medium consisting of an aggregate of these particles shows a negative permeability region near and above the resonance frequency. In this region, magnetic susceptibilities below −1 are possible. A combination of the artificial media proposed in Refs. 2 and 3 has been experimentally demonstrated to be a *left-handed* artificial medium, i.e., a medium having, simultaneously, negative electric permittivity and negative magnetic permeability.[4–6] On the other hand, embedding metallic resonant particles showing cross polarization effects (i.e., an electric polarization as a response to an applied magnetic field and vice versa) in a host dielectric medium is the usual technology for obtaining bi-isotropic and/or bianisotropic artificial media (i.e., media which replicate optical activity at microwave frequencies).[7–10] Indeed, all the aforementioned artificial materials (bi-isotropic, bianisotropic, NMPM, and left-handed materials) turn out to be very similar in many aspects. Thus, the presence of resonances in the commonly used bianisotropic and bi-isotropic inclusions suggests the existence of regions with negative permeability and/or permittivity, at least if losses are very low or, simply, ignored. Conversely, cross polarization effects could also be expected in some of the proposed resonant particles used to manufacture NMPM and left-handed materials. Our aim in this paper is to discuss the presence and effects of bianisotropy in some of the artificial NMPM and left-handed materials already proposed by other authors. We have developed for this purpose an analytical approximate model of the media accounting for bianisotropic effects. The model has been used to evaluate the magnitude of the cross polarization effects. The qualitative and quantitative results obtained from this model corroborate the main conclusions reported in Refs. 3 and 4. Moreover, the bianisotropic effects incorporated in the model explain some effects observed in the electromagnetic-wave propagation through the aforementioned media, which cannot be fully understood at the light of the theory proposed in Refs. 3 and 4.

II. APPROXIMATE ANALYSIS OF THE SRR PARTICLE

The SRR particle used for designing the NMPM (Ref. 3) and the left-handed material[4] under study is shown in Fig. 1. It is formed by two coupled conducting rings printed on a dielectric slab of thickness t. As far as the size of the particle is much smaller than the free space wavelength at resonance (in our case the particle size is about one-tenth of that
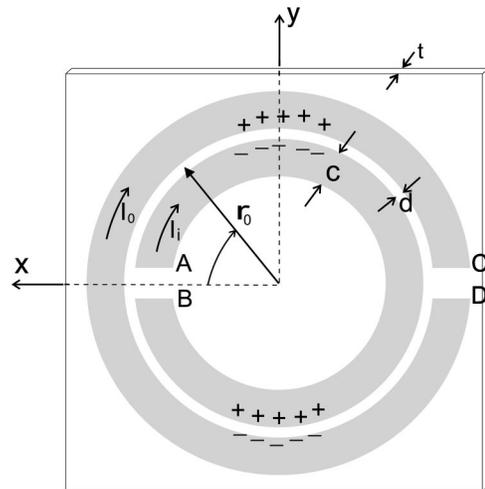

FIG. 1. The split ring resonator (SRR). For numerical calculations we have chosen the same dimensions as in Refs. 4 and 5, i.e., $c=0.8$ mm, $d=0.2$ mm, $r_0=2.3$ mm, and $t=0.216$ mm. The relative permittivity of the dielectric layer is $\epsilon_r=3.4$.

wavelength[4]), a quasistatic analysis is plausible. Under such an assumption, we will analyze the behavior of the particle when an external magnetic field $\mathbf{B} = B_z^{ext}\exp(i\omega t)\hat{\mathbf{z}}$ is applied. In that case an electromotive force $\mathcal{E} \simeq -i\omega\pi r_0^2 B_z$ is induced along the rings which is responsible for creating a current flow which produces a total magnetic moment in the particle. The slot between the rings acts as a distributed capacitance, which stores the same amount of charge (but of opposite sign) at both sides of the slot. From charge conservation,

$$\frac{dI}{d\phi} \simeq -i\omega r_0(\lambda_i + \lambda_0) = 0, \qquad (1)$$

where I is the total current flowing on both rings and λ_i and λ_o are the per unit length (p.u.l.) charge at the inner and outer rings, respectively. Equation (1) shows that the total current on the SRR does not depend on ϕ. However, the currents supported by the inner, I_i, and the outer, I_o, rings are, of course, functions of ϕ satisfying the following equation:

$$\frac{dI_{i,o}}{d\phi} \simeq -i\omega r_0\lambda_{i,o} = -i\omega r_0 C(V_i - V_o), \qquad (2)$$

where C is the p.u.l. capacitance between the rings and $V_{i,o}$ are the quasistatic voltages along the inner and outer rings respectively. The quasistatic voltages at the points marked A, B, C, and D in Fig. 1 can be obtained using Faraday's law:

$$V_A = V_D = -V_B = -V_C \simeq i\frac{\omega}{2}(LI + \pi r_0^2 B_z^{ext}), \qquad (3)$$

where L is the total inductance of the SRR. The variation of the quasistatic voltage drop along the slot could be obtained by applying transmission line theory. However, as far as the size of the particle is small with respect to the free space wavelength, a first-order approach that considers a linear variation with ϕ of V_i and V_o is justified. Considering lossless rings and using this approximation, together with Eqs. (1)–(3), the analysis shows that there is an approximately constant voltage drop, $V_i(\phi) - V_o(\phi) = \Delta V$, across the upper half of the slot ($0 < \phi < \pi$) whereas, from the symmetry of the particle, the voltage drop across the lower half of the slot is just the opposite [i.e., $V_i(\phi) - V_o(\phi) = -\Delta V$ for $\pi < \phi < 2\pi$]. The analysis also shows that the particle has a resonance at the angular frequency

$$\omega_0^2 \simeq \frac{2}{\pi r_0 CL}; \qquad (4)$$

i.e., the SRR essentially behaves as a resonant LC circuit. A more involved analysis using transmission line theory without approximations yields the same results. This result is also consistent with those obtained in Ref. 3 if we assume $L \sim \mu_0 r_0$. This assumption will be justified in the following.

The quasistatic analysis also accounts for the magnetic moment $m_z = \pi r_0^2 I$ of the particle, which is given by

$$m_z = \alpha_{zz}^{mm} B_z^{ext}, \qquad \alpha_{zz}^{mm} \simeq \frac{\pi^2 r_o^4}{L}\left(\frac{\omega_0^2}{\omega^2} - 1\right)^{-1}. \qquad (5)$$

Equation (5) shows that the particle is diamagnetic above the resonance frequency. Until this point our analysis does not essentially differ from that in (Ref. 3). However, a careful consideration of the behavior of the particle shows that the SRR should act not only as a magnetic dipole, but also as an electric dipole. This behavior is expected from the fact that quasistatic potentials and charges for $\pi < \phi < 2\pi$ are the electrical images of these quantities for $0 < \phi < \pi$, as is sketched in Fig. 1, so that the particle has a nonzero dipolar electric moment along the y direction. After some calculations, this electric dipole is found to be

$$p_y = i\alpha_{yz}^{em} B_z^{ext}, \qquad \alpha_{yz}^{em} = 2\omega_0\pi r_0^3 C_0 d_{eff}\frac{\omega_0}{\omega}\left(\frac{\omega_0^2}{\omega^2} - 1\right)^{-1}, \qquad (6)$$

where C_0 is the p.u.l. capacitance between the rings when the dielectric is removed, and the *effective* distance d_{eff} gives the p.u.l. polarization P_r along the slot as $P_r = d_{eff}\lambda_i \approx d_{eff}C_0(V_i - V_o)$ for $0 < \phi < \pi$. Here C_0 is used instead of C because it is the total (free plus polarization) charge, which contributes to the particle polarizability.

From application of the well-known Onsager symmetry principle to Eqs. (6), it can be inferred that the analyzed SRR also will show an additional cross polarizability, resulting in an induced magnetic moment when an external electric field, with the appropriate polarization, is applied. This cross polarizability could be obtained by direct calculations. However, since the SRR is made with reciprocal media, reciprocity should also hold for the whole structure. In that case, from the symmetry relations for the generalized susceptances[11,12] and Eqs. (6), the aforementioned cross polarizability can be shown to be given by

$$m_z = i\alpha_{zy}^{me} E_y^{ext} = -i\alpha_{yz}^{em} E_y^{ext}, \qquad (7)$$

where E_y^{ext} is an applied external electric field directed along the y axis of the particle and α_{yz}^{em} is given by Eqs. (6).

The particle also has an α_{xx}^{ee} polarizability, which can be approximately evaluated as the polarizability of a disk,[12]

$$\alpha_{xx}^{ee} \simeq \epsilon_0 \frac{16}{3} r_{ext}^3; \qquad r_{ext} = r_0 + c + d/2 \qquad (8)$$

as well as a polarizability α_{yy}^{ee} which is given by

$$\alpha_{yy}^{ee} = \alpha_{xx}^{ee} + 4\omega_0^2 r_0^2 C_0^2 L d_{eff}^2\left(\frac{\omega_0^2}{\omega^2} - 1\right)^{-1}. \qquad (9)$$

The second term on the right-hand side of Eq. (9) is calculated from Eq. (7), which implies that any external field E_y^{ext} will induce a current on the ring which, in turn, will create an electric polarization, which cannot be neglected around the resonance frequency. Finally, Eqs. (5)–(9) are summarized as follows:

$$p_x = \alpha_{xx}^{ee} E_x^{ext}, \qquad (10)$$

$$p_y = \alpha_{yy}^{ee} E_y^{ext} + i\alpha_{yz}^{em} B_z^{ext}, \qquad (11)$$

$$m_z = -i\alpha_{yz}^{em} E_y^{ext} + \alpha_{zz}^{mm} B_z^{ext}, \tag{12}$$

which clearly shows the bianisotropic behavior of the particle. From Eqs. (10)–(12) it should be possible, after application of an appropriate homogenization procedure, to obtain the macroscopic susceptances of an *effective* continuous medium consisting of a random or periodic arrangement of these particles. The suitability of such a homogenization procedure will be mainly limited by the electrical size of the unit cell. There exists wide experimental evidence of an appropriate homogenization procedure that provides a good description of the main features of the electromagnetic behavior of left-handed and/or bi(iso/aniso)tropic metamaterials, provided that the size of the unit cell is smaller than approximately one-tenth of the free space wavelength—as is the case—or even more.[4,6,9,10] Losses can also play an important role in the homogenization procedures, but the numerical simulations reported in Ref. 4 show that, for the particular structure analyzed here, the main experimental results can be accounted for by neglecting losses in the analysis of the artificial atoms. Furthermore, although losses are systematically neglected along this paper, they could be easily incorporated in the proposed model by simply adding a frequency-dependent imaginary part $-iR/\omega$ to the inductance L (accounting for the series resistance R of the metallic strips) and an imaginary part $i\omega G$ to the p.u.l. capacitance C (accounting for the p.u.l. shunt conductance G across the slot between the rings).

III. CONSEQUENCES AND QUALITATIVE EVIDENCE OF BIANISOTROPY

In order to evaluate the physical implications of the bianisotropic nature of the SRR particle, we have analyzed both the anisotropic NMPM proposed in Ref. 3 and the two-dimensional left-handed medium proposed in Ref. 4. The first medium consists of a number of identical SRR particles printed on a dielectric slab (relative dielectric permittivity ϵ_r and thickness t) and arranged in a cubic lattice with spacing a. The left-handed material[4] is formed by placing between the SRR particles of the above medium wires of (equivalent) infinite length, which are parallel to the y axis of these particles [see the inset in Fig. 2(c) in Ref. 4]. The wire medium behaves as an anisotropic plasma, with $\epsilon_{yy} = \epsilon_0(1 - \omega_p^2/\omega^2)$, ω_p being the plasma frequency.[1,4] Neglecting losses and taking into account the constraints imposed by the reciprocity theorem,[13] the constitutive relations for these media can be written as

$$\mathbf{D} = \epsilon_0(1 + \bar{\bar{\chi}}_e) \cdot \mathbf{E} - i\sqrt{\epsilon_0 \mu_0} \bar{\bar{\kappa}} \cdot \mathbf{H}, \tag{13}$$

$$\mathbf{B} = i\sqrt{\epsilon_0 \mu_0} \bar{\bar{\kappa}}^T \cdot \mathbf{E} + \mu_0(1 + \bar{\bar{\chi}}_m) \cdot \mathbf{H}, \tag{14}$$

where, accordingly to Eqs. (10)–(12), only χ_{eyy}, χ_{exx}, κ_{yz}, and χ_{mzz} are different from zero. When losses are neglected all these quantities are real numbers.

It can be easily realized that plane transverse electromagnetic (TEM) waves can propagate along the x axis in an homogeneous medium described by the constitutive relations (13) and (14) (with the aforementioned restrictions), pro-

vided that $\mathbf{E}$ and $\mathbf{H}$ are polarized along the y and z axes of the SRR's, respectively. The wave number of these TEM plane waves is given by

$$k_x = \omega\sqrt{\mu_{zz}\epsilon_{yy} - \mu_0\epsilon_0\kappa_{yz}^2}, \tag{15}$$

which differs from the expressions in Refs. 3 and 4 because of the presence of the bianisotropic term κ_{yz}. Note that a very important consequence of Eq. (15) is the existence of a forbidden band at those frequencies satisfying

$$\mu_{zz}\epsilon_{yy} - \mu_0\epsilon_0\kappa_{yz}^2 < 0, \tag{16}$$

while transmission is possible for

$$\mu_{zz}\epsilon_{yy} - \mu_0\epsilon_0\kappa_{yz}^2 > 0. \tag{17}$$

Using Eq. (15) for the TEM wave number instead of the simplified equation $k_x = \omega\sqrt{\mu_{zz}\epsilon_{yy}}$ (Refs. 3 and 4) leads, of course, to quantitatively different results, but also to a meaningfully different *qualitative* behavior. Assuming that the NMPM has a positive dielectric constant ($\epsilon_{yy}^{NMPM} > 0$) in the whole frequency range of interest, assuming that the composite SRR and wire medium (i.e., the left-handed material) has a negative dielectric constant at the same frequencies ($\epsilon_{yy}^{LH} < 0$), and assuming that the magnetic properties of both media are identical[3,4] ($\mu_{zz}^{NMPM} = \mu_{zz}^{LH}$ and $\kappa_{yz}^{NMPM} = \kappa_{yz}^{LH}$), the simplified relation $k_x = \omega\sqrt{\mu_{zz}\epsilon_{yy}}$, which neglects bianisotropy—i.e., the magnetoelectric coupling in the SRR—predicts a forbidden band for the NMPM which *exactly* coincides with the transmission band for the left-handed material. The use of Eqs. (15)–(17), however, predicts a mismatch between the aforementioned frequency bands as far as $\kappa_{yz} \neq 0$. This mismatch would be located at the upper limit of both bands, where μ_{zz} approaches to zero (the lower limit is at the resonance, where $\mu_{zz} \to -\infty$). This mismatch, although apparently ignored in the discussion by the authors of the previously cited papers, is in fact, clearly perceivable in the numerical simulations reported in Fig. 2(c) of Ref. 4 and in the experimental curves in Fig. 3. in the same paper. In our opinion, such a mismatch cannot be explained if κ_{yz} is neglected in the dispersion relation (15); i.e., it cannot be explained if bianisotropic effects are neglected. Moreover, when numerical simulations are carried out for the same structure and for plane waves propagating in the same direction, but with the electric field polarized along the x axis of the SRR particle, the rejection band of the NMPM and the transmission band of the left-handed material exactly coincide.[5] This result can be interpreted by taking into account that the cross polarization α_{xz}^{em} vanishes in the SRR particle and, therefore, the coupling parameter κ_{xz} must vanish in the corresponding effective medium. We can thus conclude that the presence of bianisotropy provides an explanation of some, in other way unexplained, qualitative results of the numerical simulations and experiments presented in Refs. 4 and 5.

IV. NUMERICAL AND EXPERIMENTAL EVIDENCE OF BIANISOTROPY

Once it has been shown that the consideration of the magneto electric coupling (i.e., the bianisotropy nature of the artificial medium) can account for some significant qualitative features of the propagation of electromagnetic waves through the NMPM and left-handed materials under study, quantitative agreement between our model and the numerical simulations and experiments in Ref. 4 will be discussed in this section. For this purpose, the polarizabilities (10)–(12) must be calculated for the SRR particles used in Ref. 4. The p.u.l. capacitances C and C_0 have been calculated using the routines reported in Ref. 14. It is not a simple task to develop an analytical model for the total inductance L. Due to this reason, we have deduced the value of L from the experimental value of the resonance frequency for a single particle reported in Ref. 4 ($f=4.845$ GHz) and from Eq. (4). This leads, for the particular case treated in Ref. 4, to the value $L=3.03\mu_0 r_0$ (which is of the same order than the value obtained for the inductance of a ring of radius r_0 made with a wire of radius $c/2$ (Ref. 12): $L=\mu_0 r_0[\ln(16r_0/c)-2]$ $=1.87\mu_0 r_0$). Finally, the *effective* distance d_{eff} has been approximated as $d_{eff}\simeq c+d$. Using these values in Eqs. (5)–(9), the polarizabilities (10) and (11) have been calculated. Once these polarizabilities are known, the constitutive parameters of the effective medium can be obtained by means of a homogenization procedure. A rough approach is to simply take for the nonzero macroscopic susceptibilities χ_{eyy} $=\alpha_{yy}^{ee}/a^3$, $\chi_{exx}=\alpha_{xx}^{ee}/a^3$, $\kappa_{yz}=\sqrt{\mu_0/\epsilon_0}\alpha_{zy}^{me}/a^3$, and χ_{mzz} $=\mu_0\alpha_{zz}^{mm}/a^3$, where a^3 is the volume of the unit cell. This approach, which neglects the electromagnetic coupling between the individual atoms of the metamaterial, only qualitatively accounts for the behavior of the analyzed medium (for which $a=8$ mm). Just approximate qualitative results can be expected from this method, which we will call procedure No. 1. A second scheme, which we will call procedure No. 2, is based on the well-known Lorentz approach for the *local* fields on the particle: $\mathbf{E}_l=\mathbf{E}+\mathbf{P}/(3\epsilon_0)$ and $\mathbf{H}_l=\mathbf{H}+\mathbf{M}/3$. Results obtained by using this latter approach, whose main guidelines are summarized in Ref. 10, are expected to be closer to the results of the numerical simulation. Nevertheless, it is known that this approach should fail near the resonance frequencies and when applied to dense media, as is the case. Therefore results obtained following any of the procedures above are expected to agree just roughly with the experiments, but procedure No. 2 is expected to be better than procedure No. 1.

Figure 2 shows the results obtained following the procedure Nos. 1 and 2 in this paper as well as those obtained from the numerical simulation in Ref. 4. Note that the numerical simulations presented in Ref. 4 were carried out by using a commercial electromagnetic mode solver which, obviously, considers the discrete nature of the metamaterials. Therefore, although bianisotropy is not explicitly incorporated in the macroscopic constitutive relations proposed in Ref. 4, the numerical simulations (which ignore any *a priori* hypothesis about the nature of the metameterial) implicitly will account for its effect, provided it is actually present.
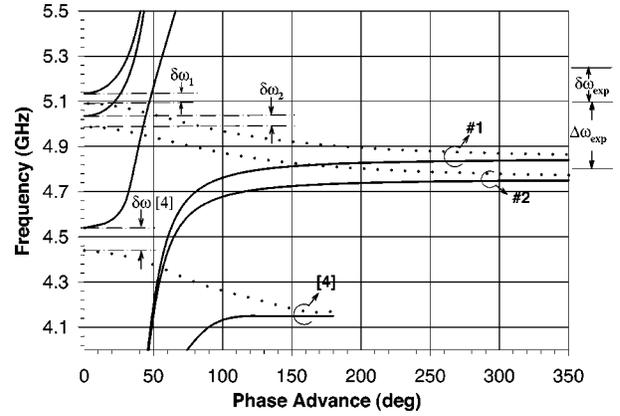

FIG. 2. Phase advance ($k_x a$) as a function of frequency for the NMPM (solid lines) and the left-handed (dotted lines) metamaterials reported in Refs. 4 and 5 for a TEM wave polarized with the electric field along the x axis and the magnetic field along the z axis of Fig. 1. The dimensions of the SRR's are as in Fig. 1. a $=8$ mm. The characteristics of the wire medium can be found in Ref. 4. Curves labeled No. 1, No. 2, and [4] show the results obtained following the two analytical methods (No. 1, No. 2) reported in this paper and the results of the numerical simulations in Fig. 2(c) of Ref. 4. The frequency gaps for which transmission is not possible neither in the NMPM nor in the left-handed metamaterial are labeled as $\delta\omega_1$, $\delta\omega_2$, $\delta\omega$ [4], and $\delta\omega_{expt}$. The experimental 3 dB transmission band for the left-handed metamaterial is shown as $\Delta\omega_{expt}$.

Although qualitative and quantitative agreement between our analytical model and the numerical simulations is just as good as can be expected from the rough approximations we have used, it is physically meaningful to predict a *gap* of frequencies, $\delta\omega$, for which propagation is not possible neither in the NMPM nor in the *left-handed* metamaterial. The gap appears in both analytical ($\delta\omega_1$ and $\delta\omega_2$) and numerical results ($\delta\omega$ [4]) and is highlighted in Fig. 2. This gap is clearly perceivable too in the experimental results depicted in Fig. 3 of Ref. 4). For comparison purposes, the measured 3 dB passband of the left-handed metamaterial, $\Delta\omega_{expt}$, and the 3 dB forbidden frequency gap, $\delta\omega_{expt}$, for both the NMPM and left-handed metamaterial have been depicted in Fig. 2. Our rough analytical models reasonably predict the position and order of magnitude of the forbidden frequency gap. This detail of the phenomenon, which is present in both experiment and numerical simulations, cannot be explained by just characterizing the NMPM by means of a negative permeability and/or the left-handed material by means of a simultaneously negative dielectric permittivity and magnetic permeability. However, it is perfectly accounted for by means of the hypothesis of the bianisotropic nature of the material.

Moreover, it was already noted that, for the case of plane waves propagating along the y axis of the SRR's, with the $\mathbf{E}$ and $\mathbf{H}$ fields polarized along the x and z axes of the SRR's, respectively, numerical simulations do not predict any mismatch between the NMPM forbidden band and the left-handed medium passband.[5] Since the cross polarizations α_{xz}^{em}

and α_{zx}^{em} vanish for the SRR particle, it is obvious that our analytical model does not predict a mismatch either. This is an additional confirmation of the hypothesis of bianisotropy as the explanation for the behavior of these media. A final evidence in favor of the theory in this paper is that, for plane waves traveling along the z axis of the SRR's, with the fields **E** and **H** polarized along the y and x axes of the particles, numerical simulations predict a narrow transmission frequency band for the left-handed material just below the resonance [see Fig. 2(d) in Ref. 4]. This result is also coherent with Eq. (9). Indeed, this equation predicts a resonance in α_{yy}^{ee} which produces very large and positive values of this polarizability just below the resonance. These high values would result in large and positive values of the dielectric permittivity of the NMPM, which, eventually, would cancel the negative values of the dielectric permittivity of the wire medium, thus giving a positive global dielectric permittivity for the left-handed material. Since the permeability of the NMPM is positive below the magnetic resonance frequency, this results in a narrow passband for the composite left-handed material at these frequencies. Once again our hypothesis seems to be confirmed by numerical simulation.

From the quantitative point of view adopted in this section some discrepancies can be observed between our model and the numerical simulations and experiments reported in Ref. 4, which deserve some comments. Thus, in numerical simulations the frequency gap is of about 100 MHz, whereas the analytical model predicts a *gap* of about 50–60 MHz. Moreover, the graphics in Fig. 2, although similar, show a systematic displacement in frequency. These discrepancies between the numerical simulations and the analytical model might be due to the limitations of the homogenization procedure and/or the numerical simulations or to the presence of spatial dispersion, which cannot be taken into account by the assumed local constitutive relations (13) and (14). Some degree of inaccuracy in the numerical simulations cannot be discarded, since the location of the experimental pass and forbidden bands shown in Fig. 2 is better reproduced by the analytical models in this paper than by the numerical simulations. Note that the bandwidths calculated from the analytical models are smaller than the experimental bandwidths. This discrepancy could be attributed to Ohmic losses, which are not taken into account in our model.

V. AVOIDING BIANISOTROPY

Since bianisotropy might be an undesired property of the medium, a method to eliminate it could be of interest. There is a slight modification of the SRR particle which would eliminate the magnetoelectric coupling of the SRR particle (and then the bianisotropy of the artificial medium) while keeping all its other interesting features. This modification consists in replacing one of the rings (the internal ring, for instance) by another ring located just behind the external ring, at the opposite side of the dielectric substrate, with the slits still placed at opposite sides. This modification of the SRR particle is sketched in Fig. 3. The electromagnetic behavior of this modified SRR (MSRR) should be in many essential aspects similar to that of the SRR shown in Fig. 1.
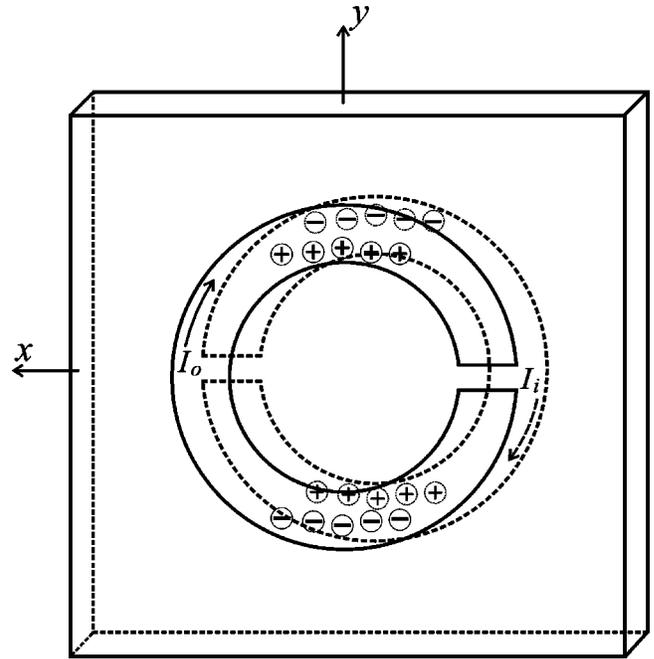

FIG. 3. The modified split ring resonator (MSRR) proposed as an alternative to the conventional SRR in order to avoid bianisotropic effects.

In particular, when a time-harmonic varying external magnetic field is applied along the z axis of the particle, it will induce—by Faraday's law—electric currents on the metallic rings with a behavior described by Eqs. (1)–(4), where now L should be the total inductance of the MSRR and C the p.u.l. capacitance between the two opposite metallic strip rings. Therefore, the MSRR shows a magnetic polarizability also given by Eq. (5) with the aforementioned new interpretation for L and C. However, as can be easily seen by inspection of Fig. 3, the electric charge is distributed on both rings of the MSRR in such a way that no net electric polarization is produced. In fact, as is sketched in Fig. 3, the electric polarization of the upper half side ($y > 0$) of the MSRR must be just the opposite of the polarization of its lower half side ($y < 0$), in order to allow the field displacement current to close the ohmic current lines. That is, the MSSR is not a bianisotropic particle.

Apart from the absence of magnetoelectric coupling, the MSRR presents an interesting additional advantage. Since the p.u.l. capacitance between the broadside coupled metallic strips of the MSRR can be made considerably higher than the p.u.l. capacitance between the edge coupled split rings (by simply widening the strips and/or by using a very thin dielectric slab and/or increasing its dielectric permittivity), it is expected that the resonant frequency (4) could be meaningfully reduced (the total size of the particle remaining unchanged) with respect to the SRR configuration. This will result in a smaller overall electrical size of the particle at the frequencies of operation of the resulting NMPM and/or left-handed metamaterials. This is a very important aspect if the artificial discrete medium has to be described as an effective continuous medium at microwave frequencies.

VI. CONCLUSIONS

The recently reported artificial negative magnetic permeability media and left-handed metamaterials have been revisited at the light of the theory of bi(iso/aniso)tropic artificial media. The conclusions obtained from this analysis complement the results of the aforementioned previous works, explaining some relevant features of the electromagnetic behavior of such media. It has been highlighted that the electromagnetic behavior of artificial bianisotropic media, NMPM, and left-handed metamaterials, made with resonant metallic inclusions in a host uniform medium, present noticeable similarities. In particular, the bianisotropic characteristics of recently reported NMPM and left-handed metamaterials have been investigated. An analytical model, accounting for magnetoelectric coupling, has been proposed for the split ring resonator (SRR), which is the elementary atom of the aforementioned NMPM and left-handed metamaterials. That coupling is responsible for the bianisotropic behavior of the equivalent continous medium consisting of an aggregate of those particles. Considering bianisotropy, some up-to-date unexplained features of the electromagnetic waves propagating through those media can be explained. In particular, it has been shown that the transmission and forbidden frequency bands for those materials can be more adequately described accounting for bianisotropy. Finally, a new modified split ring resonator, which does not present bianisotropic effects, has been proposed. This new MSRR could be useful in the design of new nonbianisotropic NMPM and left-handed metamaterials.

*Electronic address: marques@us.es

†Electronic address: medina@us.es

[1] J. Pendry, A. Holden, W. Stewart, and I. Youngs, Phys. Rev. Lett. **76**, 4773 (1996).

[2] J. Pitarke, F.G. a Vidal, and J. Pendry, Phys. Rev. B **57**, 15 261 (1998).

[3] J. Pendry, A. Holden, D. Robbins, and W. Stewart, IEEE Trans. Microwave Theory Tech. **47**, 2075 (1999).

[4] D. Smith, W. Padilla, D. Vier, S. Nemat-Nasser, and S. Schultz, Phys. Rev. Lett. **84**, 4184 (2000).

[5] D. Smith, W. Padilla, D. Vier, R. Shelby, S. Nemat-Nasser, N. Kroll, and S. Schultz, in *Photonic Crystals and Light Localization in the 21st Century*, Proceedings of the NATO–ASI Conference on Photonic Crystals and Light Localization, Crete (Greece), June 18–30, 2000, edited by Costas M. Soukoulis (Kluwer Academic, Dordrecht, 2001), p. 351.

[6] R. Shelby, D. Smith, and S. Schultz, Science **292**, 77 (2001).

[7] K. Lindmann, Ann. Phys. (Leipzig) **63**, 621 (1920).

[8] M.M.I. Saadoun and N. Engheta, Microwave Opt. Technol. Lett. **5**, 184 (1992).

[9] F. Mariotte, S. Tretyakov, and B. Sauviac, Microwave Opt. Technol. Lett. **7**, 861 (1994).

[10] A. Bahr and K. Clausing, IEEE Trans. Microwave Theory Tech. **42**, 1592 (1994).

[11] L. Landau and E. Lifshitz, *Statistical Physics*, 3rd ed. (Pergamon Press, Oxford, 1980).

[12] L. Landau and E. Lifshitz, *Electrodynamics of Continuous Media*, 2nd ed. (Pergamon Press, Oxford, 1984).

[13] C. Krowne, IEEE Trans. Antennas Propag. **32**, 1224 (1994).

[14] J. Bernal, F. Medina, and M. Horno, IEEE Trans. Microwave Theory Tech. **45**, 1619 (1997).